A Chimeric NiFe Hydrogenase Heterodimer to Assess the Role of the Electron Transfer Chain in Tuning the Enzyme's Catalytic Bias and Oxygen Tolerance

Andrea Fasano, Chloé Guendon, Aurore Jacq-Bailly, Arlette Kpebe, Jérémy Wozniak, Carole Baffert, Melisa Del Barrio, Vincent Fourmond, Myriam Brugna, Christophe Léger

A chimeric NiFe hydrogenase heterodimer to assess the role of the electron transfer chain in tuning the enzyme's catalytic bias and oxygen tolerance

Andrea Fasano [a], Chloé Guendon [a], Aurore Jacq-Bailly [a], Arlette Kpebe [a], Jérémy Wozniak [a], Carole Baffert [a], Melisa del Barrio [a,b], Vincent Fourmond [a], Myriam Brugna [a]*, Christophe Léger [a]*

a. Laboratoire de Bioénergétique et Ingénierie des Protéines. CNRS, Aix Marseille Université, UMR 7281. Marseille. France.

b. Department of Analytical Chemistry, Faculty of Chemistry, Complutense University of Madrid, 28040 Madrid, Spain.

* mbrugna@imm.cnrs.fr, leger@imm.cnrs.fr

Abstract

The observation that some homologous enzymes have the same active site but very different catalytic properties demonstrates the importance of long-range effects in enzyme catalysis, but these effects are often difficult to rationalize. The NiFe hydrogenases 1 and 2 (Hyd 1 and Hyd 2) from *E. coli* both consist of a large catalytic subunit that embeds the same dinuclear active site and a small electron-transfer subunit, with a chain of three FeS clusters. Hyd 1 is mostly active in H_2 oxidation and resistant to inhibitors, whereas Hyd 2 also catalyzes H_2 production and is strongly inhibited by O_2 and CO. Based on structural and site-directed mutagenesis data, it is currently believed that the catalytic bias and tolerance to O_2 of Hyd 1 are defined by the distal and proximal FeS clusters, respectively. To test these hypotheses, we produced and characterized a hybrid enzyme made of the catalytic subunit of Hyd 1 and the electron transfer subunit of Hyd 2. We conclude that catalytic bias and sensitivity to CO are set by the catalytic subunit, rather than by the electron transfer chain. We confirm the importance of the proximal cluster in making the enzyme Hyd 1 resist long term exposure to O_2, but we show that other structural determinants, in both subunits, contribute to O_2 tolerance. A similar strategy based on the design of chimeric heterodimers could be used in the future to elucidate various structure-function relationships in hydrogenases and other multimeric metalloenzymes, and to engineer useful hydrogenases that combine the desirable properties of distinct, homologous enzymes.

Introduction

Nature provides an infinite playground for studying long range effects in catalysis by examining how the catalytic properties of enzymes depend on structural features that are remote from their active site. In these investigations, the comparison of homologous enzymes, which share the same active site and active site environment but exhibit different catalytic properties, may be very informative.[1]

Here we shall focus on two catalytic properties that vary across homologous enzymes, and are particularly important because they may define whether a particular enzyme can be used in a particular process. Tolerance to oxygen is required for most practical applications, and it is an issue for the enzymes that catalyze reductive reactions of interest in the solar-fuel fields. The 'catalytic bias' refers to whether the catalyst is more efficient in one direction of the reaction or the other, and is measured by the ratio of the maximal rates in the two directions.[2] Only recently has it become possible to design artificial *bidirectional* molecular catalysts of redox reactions,[3,4] and redox enzymes have been a source of inspiration.[2]

Here we contribute to elucidating the structural and kinetics determinants of catalytic bias and oxygen sensitivity in hydrogenases, the enzymes that oxidize or produce hydrogen. Hydrogenases belong to three phylogenetically unrelated classes of enzymes, named according to the metal content of their H_2-binding sites: the NiFe-, FeFe- and [Fe]-hydrogenases. They are present in most microorganisms and are therefore very diverse in terms of sequences, quaternary structures, cofactor contents, and, as a result, function.[5,6] Phylogenetic analyses have defined 22 types of NiFe hydrogenases.[6] Many of them can be produced as active heterodimers, although additional subunits are required *in vivo* to anchor the enzyme into the membrane. These heterodimers are soluble, globular, and consist of a large subunit, which embeds the [NiFe$(CN)_2$(CO)] active site, and a small subunit, which houses a chain of three FeS clusters that mediate long range electron transfer between the active site and the redox partner of the enzyme (or an electrode), as schematized in figure 1A.[7] The NiFe hydrogenases from groups 1b/1c (not distinguished here) and 1d are referred to as 'standard' and 'oxygen tolerant', respectively.[6] Despite their strong homology, they have completely distinct catalytic properties. The former oxidize and produce H_2 and are strongly inhibited by CO (reversibly[8]) and O_2 (in a complex manner[9]); the latter have very little activity for proton reduction at neutral pH, are insensitive to CO and can oxidize H_2 in the presence of O_2.[10] *Escherichia coli* produces 4 distinct NiFe hydrogenases,[11] including two membrane-bound, periplasmic, 'H_2-uptake' enzymes: one of the standard type (Hyd 2, group 1c)[12] and one oxygen-resistant (Hyd 1, group 1d)[13].

The environment of the NiFe active site is conserved (figure 1C), and the most obvious structural difference between standard and O_2-resistant NiFe hydrogenases is in the small electron transfer subunit (figure 1A). In standard hydrogenases, it embeds three FeS clusters, a [4Fe4S] cluster coordinated by 4 cysteine residues that is proximal to the active site (figure 1D), a medial [3Fe4S] cluster, and a distal [4Fe4S].[12] In contrast, the proximal cluster in O_2-tolerant NiFe hydrogenases is a unique [4Fe3S] cluster, coordinated to the protein by 6 cysteine residues, including C19 and C120[13,14] (figure 1B), which has unusual magnetic and redox properties,[15,16] and is synthesized by a specific biological machinery.[17]

The proximal [4Fe3S] cluster is not responsible for making O_2-tolerant hydrogenases such as Hyd 1 unidirectional: indeed, when site-directed mutagenesis is used to replace the two supernumerary cysteines around the proximal cluster with glycine residues, the resulting C19G/C120G Hyd 1 variant embeds a canonical [4Fe4S] cluster, but it is only active for H_2 oxidation, like the wild-type (WT) enzyme.[18] The high potential, medial [3Fe4S] cluster is identical in standard and O_2-tolerant hydrogenases (SI figure S18) and does not define the catalytic bias either, at least according to the results of experiments where the [3Fe4S] cluster was replaced with a low potential [4Fe4S] cluster.[19,20] Armstrong, Hexter and co-workers have hypothesized that the distal FeS cluster, the entry point for electrons in the enzyme, controls the catalytic bias, and that Hyd 1 would have very little H_2 evolution activity because the reduction potential of this cluster is higher than in standard hydrogenases (SI Table S5).[21,22] However, this hypothesis is not strongly supported by site-directed mutagenesis experiments. Parkin *et al.* showed that the mutation of a residue near the distal cluster of *E. coli* Hyd 1 (R193L) makes its reduction potential ≈ 60 mV more negative and does increase the catalytic bias in the direction of H_2 production (by a factor of ≈ 2),[23] but this effect is small compared to the one hundred fold variation expected from Hexter's theory: indeed, based on eq. 4 in ref [22], the variation in bias should equate exp(2F/RT × 0.06). A more complex model from our group, which explicitly considers intramolecular electron transfer between the redox relay and the active site,

suggests that the kinetics of intramolecular electron transfer actually matters: if intramolecular electron transfer is fast compared to active site chemistry, as is often considered to be the case,[7] the catalytic bias should be independent of the electron transfer chain.[24] Parkin *et al.* concluded from their mutagenesis study that factors other than the distal cluster must control the bias, and observed that indeed, in *E. coli* Hyd 1, it is affected by the replacement of a residue in the large, catalytic subunit.[25]

The reaction with O_2 of NiFe hydrogenases is a complex process that oxidizes the NiFe active site into a variety of inactive species, some of which reactivate upon reduction or when anaerobic conditions are recovered.[9] *E. coli* Hyd 1 and other O_2-tolerant hydrogenases, such as the membrane bound hydrogenase (MBH) from *Ralstonia eutropha*, react with O_2 to form a single inactive state (called "NiB", or "ready") that reactivates quickly upon removal of O_2. The consensus is that this behavior is related to the unusual properties of the [4Fe3S] proximal cluster, which shows two redox transitions in a narrow range of potential (SI table S5) : the [4Fe3S] cluster would protect the active site of Hyd 1 by supplying two electrons to the active site when a O_2 molecule attacks.[14,18,26,27] However, the results of site directed mutagenesis experiments do not support the causal relation between the additional one-electron oxidation at the proximal cluster and O_2-tolerance.[18] Moreover, the observation that the isolated catalytic subunit of *R. eutropha* MBH is resistant to O_2, despite lacking all accessory FeS clusters, suggests that the *large* subunit contributes to O_2-tolerance.[28]

Most attempts to understand what defines the turnover rate and catalytic bias of standard and O_2-tolerant hydrogenases have focussed on the accessory FeS clusters, in particular the proximal and distal clusters, but whether or not the electron transfer subunit actually plays that particular role remains unsettled. To map the structural determinants of catalytic bias and tolerance to O_2 in *E. coli* hydrogenases, we move away from traditional site-directed mutagenesis by using an original approach that consists in designing and characterizing a hybrid heterodimeric hydrogenase, obtained by replacing one entire subunit of the dimeric hydrogenase with that from a different enzyme, and examining the functional consequences. We call this new construct a "chimeric dimer".

Producing such chimeric dimer is challenging because the large contact surface between the two subunits of each hydrogenase (3500 $Å^2$, about half the surface of an equatorial section of the globular dimer) makes the interaction very specific.[29] However, we show below that engineering the surface of the subunits makes possible the assembly of a non-natural dimer of the large (catalytic) subunit of Hyd 1 and the small (electron transfer) subunit of Hyd 2 (figure 1A). This chimeric dimer was produced in low yields, but this is not an issue for an investigation by direct electrochemistry, a technique which is known to require very small amounts of active enzyme and gives an immediate read out of the enzyme's catalytic properties.[30,31]

Here, the comparison of the chimeric and native dimers gives unambiguous evidence that the catalytic bias and CO sensitivities of *E. coli* NiFe hydrogenases are defined by their large subunit, whereas the proximal cluster is not the unique determinant of the tolerance to O_2.

Results

Design

We produced the 'L1S2mod' chimeric heterodimer by modifying the small subunit of Hyd 2 ('S2') so that it binds the large subunit of Hyd 1 ('L1'). The choice of modifying the small subunit (rather than the large subunit or both) was arbitrary. We examined the structure of the interfaces of the two native heterodimers (PDB accession codes 3UQY and 6EHQ) to identify the interfacial side chains and

the intersubunit interactions, by using the PISA software[32] or simply by selecting all residues of the small subunit that are up to 3 Å away from the large subunit. Yellow and red dots in figure 1G and SI figure S17 mark these interfacial residues. Black dots indicate residues important for function (cf SI section S9.1). We examined all interfacial residues in the S2 subunit one at a time, aiming for the smallest number of alterations of S2 and applying specific rules to decide which residues to modify. We did not change any residue that is conserved between S1 and S2. We also decided not to alter the residues involved in conserved interactions (when *distinct* residues at the same position in S face a conserved residue in the large subunit, label "1" above the alignments in figures 1G and S17); nor the interfacial residues whose side chains point toward the small subunit and are thus unlikely to be involved in interactions (label "2"); nor the residues that are similar in S1 and S2 (label "3"); nor the residues that are either shown or suspected to be important for function according to the literature or that neighbor residues important for function (label "4"). We replaced the interfacial S2 residues that did not fall into any of the above categories with the same-position S1 residues.

Figure 1G shows a portion of the alignment of S1, S2 and the engineered small subunit S2mod (see the complete alignment in SI figure S17). Orange boxes indicate the residues of S2 altered in S2mod. Figure 1E shows an Alphafold model[33] of the structure of the chimeric dimer; orange sticks indicate the 13 residues modified in S2mod. Figure 1F shows a detail of the modified interface, with the structures of WT Hyd 1 (L1 and S1 shown in dark and light blue, respectively), WT Hyd 2 (L2 and S2 in dark and light green), and the model of L1S2mod in orange. The S2 residues E39, N40 and E44 did not fall into any of the 4 above categories and were replaced with the same position residues in S1, K, D and S, respectively (figures 1F and 1G). The S2-E39K mutation prevents a clash with the L1 D211 residue in the chimeric enzyme.

In a preliminary attempt, we could produce another active chimeric dimer with a slightly different replacement of 14 S2 residues ('S2mod1' in SI figure S17). The differences between S2mod1 and S2mod included the preservation of M94, the replacement Y256A (compared to Y256L in S2mod), the replacements H59T and N64V (not replaced in S2mod, because these residues are believed to be important for proton transfer in *D. vulgaris miyazaki*[34] and *D. gigas*[35] NiFe hydrogenases). In terms of electrochemical response, L1S2mod and L1S2mod1 gave very similar results (SI figure S15), but only the former, which gave better yield, activity (current magnitude in electrochemical experiments) and stability upon storage, is discussed hereafter.

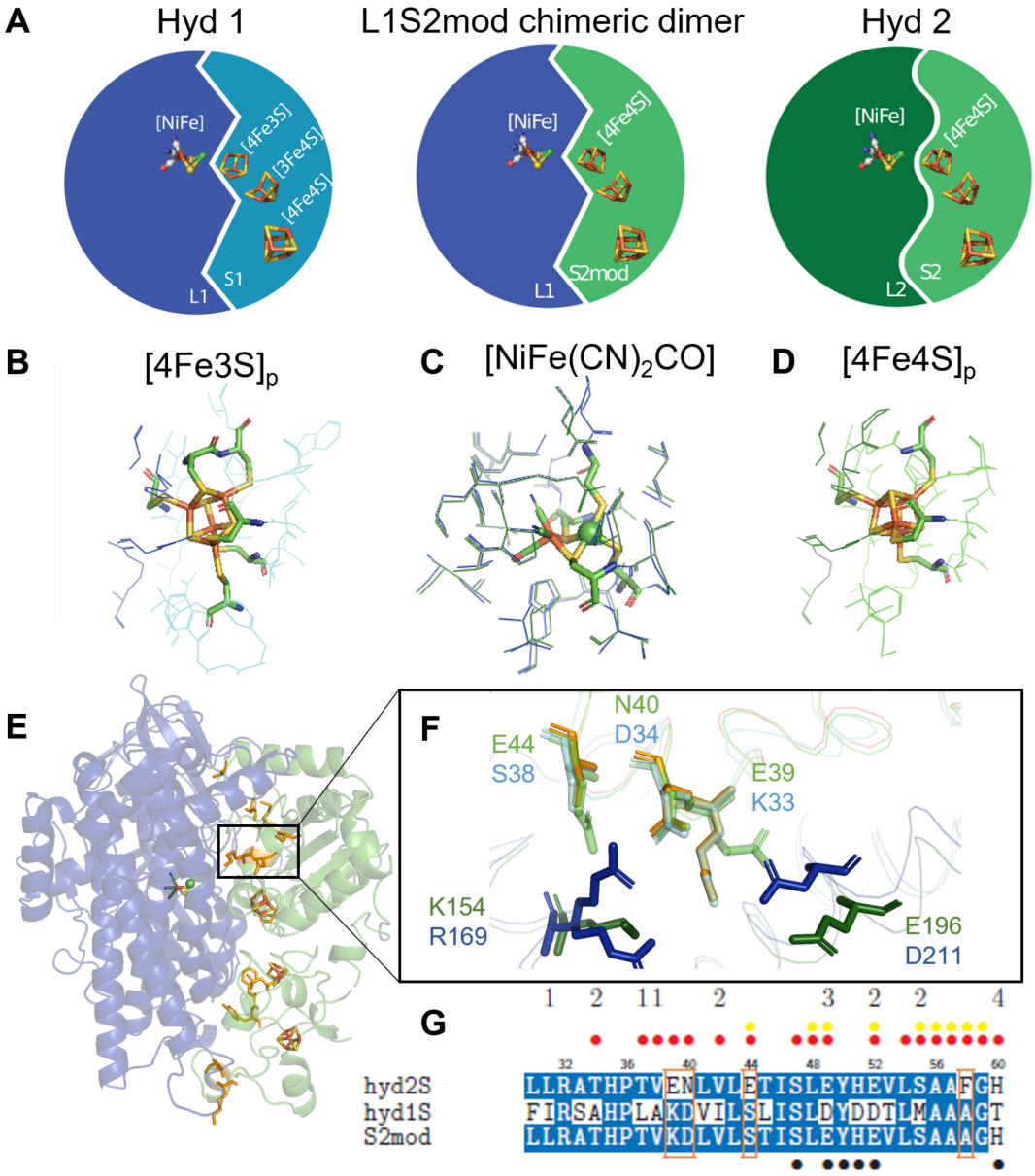

Figure 1: Structures of *E. coli* Hyd 1 and Hyd 2, and design of the L1S2mod chimeric dimer. Panel A: schematic representation of Hyd 1 and Hyd 2 WT with their cofactors and of the L1S2mod chimeric complex. Panel B: structure of the 6Cys-[4Fe3S] proximal cluster of Hyd 1, and the residues 6 Å around the cluster (dark blue: large subunit ; light blue: small subunit ; PDB 3UQY). Panel C: structure of NiFe active site [$NiFe(CN)_2(CO)$], the coordinating cysteines and the residues up to 6 Å away from the dinuclear cluster (blue: Hyd 1, PDB 3UQY ; green: Hyd 2, PDB 6EHQ). SI figure S20 shows the position of the three non-conserved residues in the environment of the active site: L1-V82/L2-T67, L1-A550/L2-S580, L1-T532/L2-S502. Panel D: structure of the 4cys-[4Fe4S] proximal cluster of Hyd 2 (PDB 6EHQ) and the surrounding residues (large subunit: dark green ; small subunit: light green). Panel E: Alphafold model of the L1S2mod chimeric complex (dark blue: L1, light green: S2) with the 13 modified S2 residues shown in orange. Panel F: detail of the interface between Hyd 1 (blue) and Hyd 2 (green, dark and light colors for the large and small subunits, respectively) and S2mod (orange). The S2 residues shown in sticks were mutated in the chimeric complex with the corresponding residues of Hyd 1. Panel G: fragment of the alignment of the sequences of the small subunits of Hyd 1, Hyd 2 and S2mod (see SI figure S17

for the entire alignment). Red and yellow bullets point to the residues at the interface between the large and small subunits. Black bullets mark residues known or predicted to be important for function (see SI tables S6 and S7). Numbers on top represent the exclusion rules we used to select the residues that we did not modify in the chimeric complex: 1/ residues that point towards conserved residues in the large subunits of Hyd 1 and Hyd 2; 2/ residues that point towards either the inside of the small subunit or the solvent; 3/ residues that are not conserved in the small subunits, but that are very similar in S1 and S2; 4/ residues that are considered important for function, or that are close to important residues. Orange boxes mark the positions of the mutations of S2mod.

Protein production

The enzyme *E. coli* Hyd 1 and the double mutant C19G/C120G[18] were produced as described in our previous work[36,37] (SI sections S4-S6), from plasmids (pET24a) in the *E. coli* FTD147 (DE3) and the *E. coli* FTD147 (DE3) Δ*recA* strains carrying chromosomal in-frame deletions of the genes encoding the large subunits of hydrogenase-1, -2, and -3.[37–40] The recombinant Hyd 1 hydrogenase was produced as a dimeric, soluble form, consisting of only a large subunit (L1, or HyaB) and a small subunit (S1, or HyaA), or L1S1. The C-terminal membrane- anchoring hydrophobic helix of S1 was replaced with a Streptag II. The yield was in the range 25-50µg per L of culture for both the WT enzyme and the C19G/C120G mutant. We produced Hyd 2 (L2S2) as described in ref [12], much more easily than with the expression system that we proposed before[37]. The yield was up to 450 µg of protein per L of culture.

We synthesized the S2mod genes, and produced the L1S2mod chimeric dimer in an engineered *E. coli* strain where we further deleted the gene encoding the small subunits of Hyd 1 (Δ*hyaA*), to prevent the association between the native forms of L1 and S1 or L2 and S2, which is natural but not desired here. We also engineered the *E. coli* strain FTD147 (Δ*iscR*) to optimize the assembly of the subunits and the production of this chimeric enzyme. The dimer was purified using a C-terminal Streptag II on S2mod. Proteomic analysis confirmed the presence of the L1 and S2mod proteins in a sample of the purified chimeric dimer (SI section S6.3). The yield was up to 55 µg of proteins per L of culture.

As negative controls, we purified the isolated L1 subunit using a N-terminal Streptag II, and observed no activity. Our attempts to produce an active complex by assembling the WT L1 and S2 subunits also failed (SI section S6.2).

Electrochemical characterization of the catalytic bias

The kinetic properties of the chimera were examined using protein film voltammetry (PFV).[30,31,41] In this technique, the enzyme is adsorbed onto an electrode and undergoes direct electron transfer with this electrode, the rotation of which prevents H_2 depletion.[42] The electrode potential can be set to a value that is higher than the Nernst potential of the H^+/H_2 couple to drive H_2 oxidation, or low enough to make the enzyme produce H_2. The catalytic reaction results in an electron flow (counted here as a negative or positive current for H_2 evolution or oxidation, respectively) that is proportional to the turnover frequency and the electroactive coverage. In a cyclic voltammetry experiment, the electrode potential is sequentially swept up and down, to observe H_2 evolution at low potential and H_2 oxidation at high potential in a single experiment. The *magnitude* of the currents observed in PFV experiments should not be considered because the amount of enzyme adsorbed on the electrode is

not controlled, cannot be measured, and varies between distinct experiments; only the *shapes* of the voltammograms matter.

Figure 2A compares the voltammetric signatures of the L1S2mod chimera (orange) and those of the WT Hyd 1 (dark blue), C19G/C120G Hyd 1 (light blue) and Hyd 2 (green) enzymes recorded at pH 6, under one atmosphere of H_2. With all enzymes under the conditions of figure 2A, a hysteresis is seen in the high potential part of the voltammogram, which reveals the reversible formation of the oxidized, inactive state of the enzyme called NiB.[10,43,44] This will be discussed in relation to oxidative inactivation below.

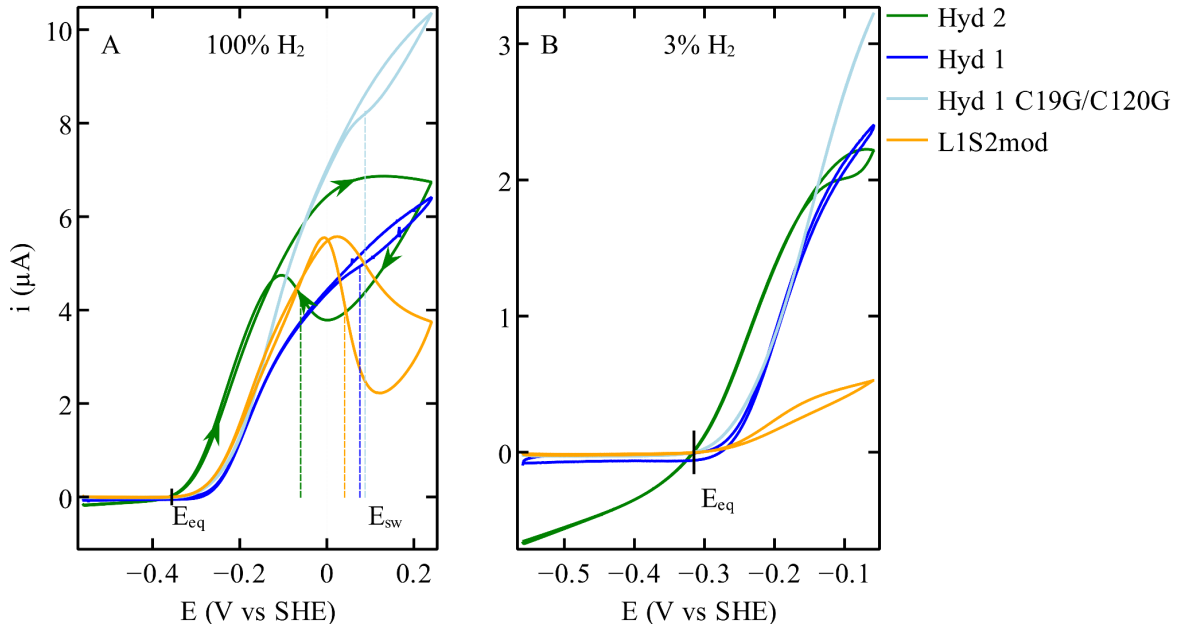

Figure 2: Cyclic voltammograms (CV) of Hyd 1 WT (blue), Hyd 2 WT (green), the chimeric NiFe L1S2mod (orange) and the Hyd 1 variant C19G/C120G (lightblue) under 100% H_2 (panel A) and 3% H_2 (panel B). In all cases, the contribution of the capacitive current was removed by subtracting a blank CV recorded with no enzyme. The signals were not scaled or normalized; note that in protein film electrochemistry, the magnitude of the signal varies between films and cannot be interpreted. However, panels A and B show CV recorded with the same films of each enzyme, so that the intensities in the two panels *can* be compared. The four panels of SI figure S16 show the CV traces at 100% and 3% H_2, one film in each panel. The colored dash lines in panel A indicate the value of the "switch potential" (E_{sw})[43,45] measured from the position of the inflexion point on each downward sweep (Hyd 1: 0.076 V; C19G/C120G Hyd 1: 0.088 V; Hyd 2 : -0.060 V; L1S2mod : 0.041 V). Experimental conditions: 40°C, pH 6, electrode rotation rate 3000 rpm, potential scan rate 20 mV/s.

Voltammograms can be used to quantify the catalytic bias of the enzyme by comparing the magnitudes of the positive and negative catalytic currents. Since H_2 evolution by NiFe hydrogenases is faster at lower pH and inhibited by the reaction product H_2,[46] the evaluation of the bias is usually performed from voltammograms recorded at low H_2 concentration and acidic pH, to facilitate the observation of the reductive activity.[10] At low H_2 concentration, care must be taken that the current is low enough that the signal is not affected by H_2 depletion near the rotating electrode (H_2 depletion results in a current that plateaus off at high potential and whose magnitude strongly depends on electrode rotation rate).

The decrease in the magnitude of the H_2 oxidation current when the H_2 concentration is decreased from 1 mM (under 1 atm. of H_2, figure 2A) to 30 µM (3% H_2, figure 2B) is greater for L1S2mod (10-fold decrease) than for Hyd 2 (3-fold decrease); this is fully consistent with the Michaelis constant for H_2 of L1S2mod being greater than that of Hyd 2 (410 ± 50 µM H_2 versus 62 ± 8 µM, at pH 6, T=40°C, see SI section S7.2).

The data in figure 2B demonstrate that the large subunit of Hyd 2 is required to make the enzyme able to catalyze H_2 evolution at a significant rate. Indeed, with all four enzymes, the oxidative current is greater than the reductive current, but only in the cases of Hyd 2 is the H_2-evolution current significant (this is also true with the standard hydrogenase from *D. fructosovorans*, Hyn, from group 1b, see SI figure S6). A quantitative analysis of the catalytic bias is provided in SI section S7.1. Lower pHs are required to observe H_2 production by Hyd 1[21], but at pH 5 and below, the films of Hyd 2 and L1S2mod were too unstable to allow comparison with Hyd 1.

CO inhibition

The sensitivity to the competitive inhibitor CO was quantified in electrochemistry experiments where the catalytic H_2 oxidation current is monitored as a function of time at a constant electrode potential, following the injection of a small amount of CO saturated solution in the electrochemical buffer (figure 3B).[8,47] The CO concentration increases instantly after the injection at t=0, then decreases exponentially, with a time constant τ, as CO is flushed away by the stream of H_2,

$$[CO] = [CO]_0 \exp(-t/\tau) \qquad \text{Equation 2}$$

where $[CO]_0$ is the CO concentration just after the injection, as schematized in figure 3A. In the case of all four enzymes considered here, CO binding and release is fast and the CO in solution therefore continuously equilibrates with the enzyme active site, so that the change in H_2-oxidation current against time after the injection is simply:

$$i = \frac{i_0}{1 + [\mathrm{CO}]_0 \exp(-t/\tau)/K_I} \qquad \text{Equation 3}$$

where i_0 is the current before the exposure to CO, and K_I the inhibition constant.[8,47]

At E = -59 mV vs SHE, 40°C, pH 6, under 1 atm. of H_2, the apparent values of K_I were: Hyd 1, 1.26 ± 0.09 mM; C19G.C120G Hyd 1, 1.09 ± 0.16 mM; L1S2mod, 0.56 ± 0.05 mM; Hyd 2, 0.055 ± 0.005 mM (SI section S7.3). Hence the inhibition strength changes in the order Hyd 1 ≈ C19G/C120G Hyd 1 ≈ L1S2mod << Hyd 2, consistent with the observation in figure 3B that Hyd 2 is much more strongly inhibited by CO than any of the other enzymes.

Since CO is a competitive inhibitor of H_2 oxidation, this K_I is an apparent value, which is greater than the true dissociation constant by a factor $1+[H_2]/K_m$, where K_m is the Michaelis constant for H_2.[47] This protective effect does not explain the observed variations in K_I: e.g. K_I is ten times smaller for Hyd 2 than L1S2mod despite K_m being smaller (62 ± 8 µM for Hyd 2, 410 ± 50 µM H_2 for L1S2mod, at pH 6, T=40°C, SI section S7.2).

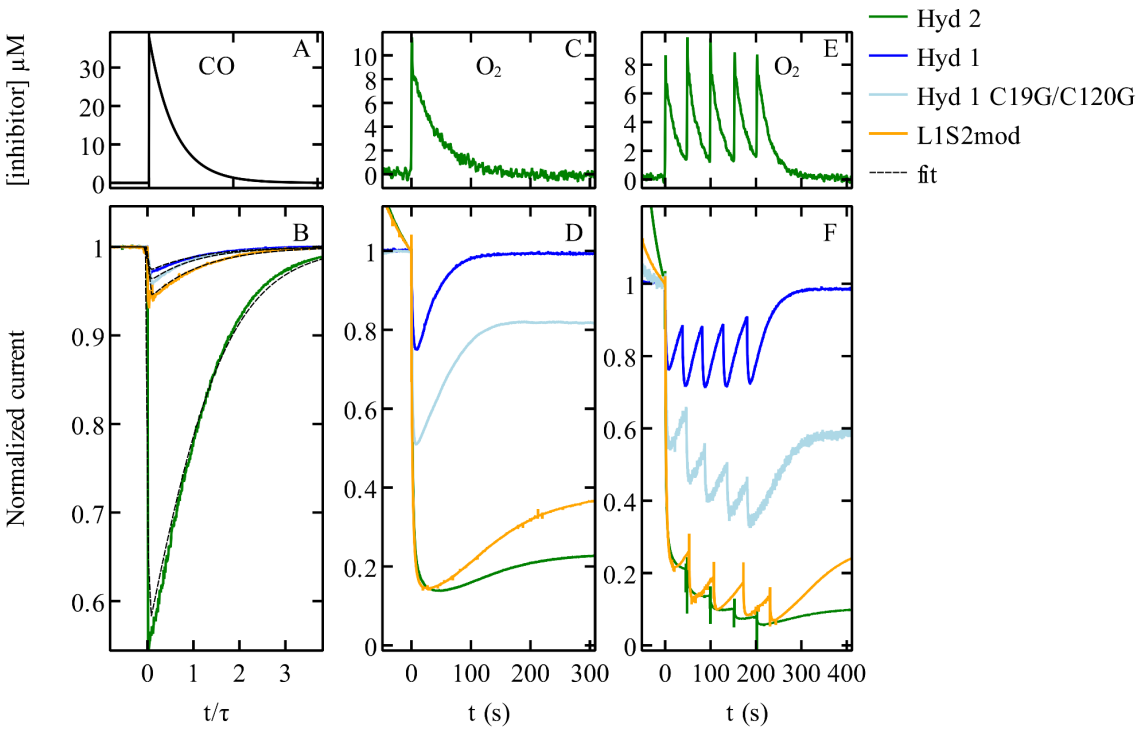

Fig 3. Chronoamperometric experiments showing the Inhibition of the four hydrogenases by CO (panels A & B), and O_2 under conditions of short and long exposures (panels C & D and E & F, respectively). The color code is Hyd 1 : dark blue ; C19G/C120G Hyd 1: light blue ; L1S2mod : orange ; Hyd 2 : green. In all cases, the electrode potential was constant and the catalytic current was monitored as a function of time, following the injection of one or several aliquots of solution saturated with CO or O_2 in the electrochemical cell. The top panels show the changes in inhibitor concentration against time.
Panel A. The change in CO concentration against time after injection is exponential, with a time constant τ (equation 2) that can be measured by analyzing the data with eq. [47]. Panel B: the corresponding change in catalytic current measured at E=-0.059 V vs SHE, against time over τ. The dashed lines show the fits of eq. 3, used to measure the inhibition constants.
Panel C: the change in O_2 concentration in one of the experiments shown in panel D, with a single injection of inhibitor, deduced from the O_2 reduction current recorded on a second working electrode[48] (see SI figure S13). Panel D: the corresponding change in H_2-oxidation catalytic current against time measured at E = 141 mV vs SHE, following a single injection of 9.6 µM O_2 in the cell and normalized by the current measured before the injection of O_2. The time constants τ were: Hyd 1: 22 s, C19G/C120G Hyd 1: 28 s, L1S2mod: 38 s, Hyd 2: 45 s.
Panel E: the change in O_2 concentration in one of the experiments shown in panel F, with multiple injections of inhibitor, deduced from the O_2 reduction current recorded on a second working electrode[48] (see SI figure S14). Panel F: the corresponding change in catalytic current against time measured at E=+0.141 V vs SHE, following a multiple injection of 8 µM O_2 in the cell and normalized by the current measured before the injections of O_2.
The time constants τ were: Hyd 1: 23 s, C19G/C120G Hyd 1 : 39 s, L1S2mod: 29 s, Hyd 2: 27 s.
All experiments at T=40°C, pH=6, 1 atm. of H_2, ω = 3000 rpm.

Oxidative inhibition

The oxidative inactivation of the enzyme is easily assessed from voltammetric experiments under anoxic conditions, by examining the redox-driven changes in activity against electrode potential

(figure 2A), and from chronoamperometric experiments where the activity is monitored as a function of time at a constant potential, after transient exposure to O_2 (figures 3D and F).

Under anoxic conditions, important information comes from examining the shape of the voltammetric response during the sweep towards low potential (marked by arrows in figure 2A), where an abrupt increase in current reveals the reactivation of the enzyme at the potential called 'E_{switch}'. The reactivation is sudden because the rate of reactivation increases exponentially as the electrode potential decreases. The faster this reactivation, the more positive the switch potential.[43,45] That E_{switch} decreases in the order Hyd 1 = C19G/C120G Hyd 1 > L1S2mod >> Hyd 2 (figure 2A) shows that the rate of reactivation increases from Hyd 2 to Hyd 1, and in particular from Hyd 2 to L1S2mod, which demonstrates the importance of the large subunit.

Experiments in figures 3D and F show the response to exposure to either a short (about 30 s, panel D) or prolonged exposure of the enzymes to O_2 (300 s, panel F). Similar experiments have been designed before to evidence the detrimental effect of the C19G/C120G mutation under conditions of long exposure to O_2[18,26]. In the experiments in figure 3, instead of setting a constant O_2 pressure as in refs [18,26], we injected either one or a series of aliquots of O_2-saturated buffer in the electrochemical cell (like we do with CO, experiments in figure 3B), and we monitor the O_2 concentration as a function of time on a 2nd working rotating electrode poised at a low potential;[48] the O_2 concentration is schematized in each panel above the current responses (see SI figures S13 and S14 for the measured time-dependent O_2 concentrations). The tolerance of the enzymes to O_2 is assessed from the amount of H_2-oxidation current that is maintained during and after exposure to O_2.

Figures 3D and F shows that all enzymes but Hyd 1 react with O_2 to form an inactive state that does not reactivate under the conditions of the experiments ; the longer the exposure, the more pronounced the loss of activity. As a consequence, long exposure experiments discriminate less between the different O_2-sensitive enzymes than short exposures.

However, in both types of experiments, the O_2-tolerance decreases in the order Hyd 1 > C19G/C120G Hyd 1 >> L1S2mod > Hyd 2, showing that most of the difference between Hyd 1 and Hyd 2 is due neither to the proximal cluster (which is a canonical [4Fe4S] cluster in both C19G/C120G Hyd 1[18] and Hyd 2) nor to the large subunit (which is the same in Hyd 1 and L1S2mod). This suggests that structural features in the electron transfer subunit other than the proximal cluster determine the O_2 tolerance of Hyd 1.

Discussion

Many distinct, homologous hydrogenases have been characterized over the last twenty years, and it became obvious that some hydrogenases are more active in one direction of the reaction than the other, or particularly O_2 resistant. In each case, understanding why this happens is a challenge. To obtain conclusive evidence about whether or not the accessory clusters of *E. coli* Hyd 1 make the enzyme more unidirectional and O_2 resistant than its homologous enzyme Hyd 2, we proposed an original approach that consists in characterizing an artificial L1S2mod chimeric dimer, obtained by assembling the large, catalytic subunit of Hyd 1 (an O_2-resistant, unidirectional enzyme) and the small, electron transfer subunit of Hyd 2 (an O_2 sensitive, bidirectional enzyme).

The data shown in this paper have been obtained with one particular version of the chimeric L1S2mod dimer, obtained by modifying 13 S2 residues located near the interface with L1. Our attempts to produce an active dimer from the native L1 and S2 proteins failed, consistent with previous investigations according to which the L1/S1 and L2/S2 interactions are specific.[29] We

produced the L1S2mod dimer in an *E. coli* strain from which the structural genes of S1 and L2 were deleted, to prevent the formation of the natural dimers. The yield was low, so crystallization was not an option, but proteomic analyses of the purified samples confirmed that the sequence of the dimer was as intended. We performed direct electrochemistry experiments[30,31] to compare the kinetic properties of the chimeric dimer with those of the native Hyd 1 and Hyd 2 enzymes.

Regarding CO inhibition, there was previous evidence that the peculiar [4Fe3S] proximal cluster in S1 is *not* the reason Hyd 1 is insensitive to CO (indeed, the C19G/C120G mutation of *E. coli* Hyd 1 had no effect on CO inhibition[18]). The comparison of Hyd 1, Hyd 2 and L1S2mod in figure 3B, showing that the strength of inhibition by CO changes in the order Hyd 1 ≈ L1S2mod << Hyd 2, demonstrates that the reaction with CO is actually independent of the entire electron transfer subunit.

We reached the same conclusion for the catalytic bias, which is similar for Hyd 1 and the L1S2mod chimeric complex (figure 2B), and thus appears to be mainly defined by the large subunit rather than the FeS clusters in the small subunit. It had already been observed that replacing the [4Fe3S] proximal cluster of Hyd 1 with a standard [4Fe4S] cluster has no effect on the catalytic bias and on the overpotential for H_2 oxidation,[18] despite the fact that it decreases the redox potential of the cluster. Based on the quantitative analysis of the steady-state CVs in SI section S7.1, we note that the L1S2mod variant does not behave exactly like Hyd 1 and we estimate that the bias of L1S2mod is less extreme than that of Hyd 1. This points to a minor effect of the electron transfer chain in defining the bias.

The above conclusion contrasts with a very common assumption according to which either the distal cluster[21] or the entire electron transfer chain defines the bias. For example, the bias in the direction of H_2 oxidation of the group 2a Huc NiFe hydrogenase from *Mycobacterium smegmatis* was recently tentatively ascribed to the presence of three high potential [3Fe4S] clusters in the electron transfer chain of this enzyme.[49] We offer an alternative explanation. In a previous study of a series of variants of the standard NiFe hydrogenase from *D. fructosovorans* (which shows the same catalytic bias as *E. coli* Hyd 2, SI figure S6), we observed that replacing a particular residue in the large subunit selectively slows H_2 production, thus increasing the bias in the direction of H_2 oxidation, and we demonstrated that this change is qualitatively consistent with H_2 release along the H_2 channel being the rate limiting step in the H_2 evolution reaction (but not in H_2 oxidation) and being slowed by the mutations.[50] The gas channel of the recently characterized *Mycobacterium smegmatis* Huc hydrogenase is actually reported to be particularly narrow, and we speculate that this feature, rather than the presence of high potential FeS clusters, may be the reason Huc has no detectable H_2 evolution activity.[49] It may also be that the large overpotential for H_2 oxidation observed in the voltammetry of Huc results from slow *interfacial* electron transfer, if the distance between the electrode and the electron transfer chain is long (this hypothesis cannot be ruled out without fitting the voltammetric waveshape[51]).

In addition to sensitivity to CO and catalytic bias, the hydrogenases 1 and 2 from *E. coli* are also notoriously distinct in terms of reactivity with O_2. O_2-tolerant NiFe hydrogenases (in group 1d) are oxidized to a unique inactive state that reactivates quickly upon removal of O_2, whereas standard hydrogenases like Hyd 2 are oxidized to a mixture of inactive states that are more difficult to reduce and reactivate. The O_2 tolerance is usually ascribed to the atypical [4Fe3S] proximal cluster in the small subunit of Hyd 1, but our data in figures 2A and 3D and F give a more complex picture.

Figure 2A compares the "switch potentials", at which the enzyme reactivates after anaerobically inactivation. This is a kinetic parameter: the higher the switch potential, the faster the

reactivation.[43,45] The reactivation rate decreases in the order Hyd 1 = C19G/C120G Hyd 1 > L1S2mod >> Hyd 2, showing that the *large* subunit of Hyd 1 is responsible for the fast reactivation of the inactive state. Note that in O_2 resistant enzymes, the same inactive state is produced upon aerobic and anaerobic inactivation, so this reactivation kinetics is also relevant to tolerance to O_2.[43]

Figure 3D shows the response of the four enzymes to a short exposure to O_2. Longer exposures give qualitatively the same results (figure 3F), except that these conditions level off the differences between the most O_2 sensitive enzymes (C19G/C120G Hyd 1, L1S2mod and Hyd 2). As emphasized before, the mutation of the proximal cluster has very little effect when the enzyme is exposed to a burst of O_2. This was discussed in terms of the cluster being useful only to prevent the formation of the inactive states other than NiB under conditions of longer exposure.[26] However, the striking difference between the responses of the C19G/C120G Hyd 1 mutant and the O_2 sensitive enzyme Hyd 2 observed in figure 3D (a control that was not shown in previous work[18,26]) reveals that structural determinants *other than the proximal cluster* are also crucial for O_2 tolerance. The comparisons between the C19G/C120G Hyd 1 mutant, the L1S2mod chimera and Hyd 2, shows that most of that difference is due to the part of the small subunit that is not the proximal cluster, with a smaller but significant effect of the large subunit (revealed by the greater tolerance of L1S2mod over Hyd 2). The latter effect may explain the observed O_2 tolerance of the isolated large subunit of *R. eutropha* MBH.[28]

More efforts will be required to precisely locate the structural determinants of O_2 tolerance in the electron transfer subunit. The contribution of the medial or distal FeS clusters cannot be excluded, although there are no experimental data to support this hypothesis yet. The environment of the medial cluster is very similar in Hyd 1 and Hyd 2 and nearly identical in Hyd 1 and the L1S2mod chimera (SI figure S18), but the solvent accessibility of the medial clusters is apparently different in O_2-tolerant and O_2-sensitive enzymes, which might influence the electrochemical potential of the cluster.[52] However, there is no clear correlation between the potential of this medial cluster and O_2-tolerance in the series of native NiFe hydrogenases for which such data are available (SI table S5). The properties of the *distal* cluster (SI figure S19) are distinct in Hyd 1 and Hyd 2, but site-directed-mutagenesis data showing that this difference defines the reaction with O_2 have not been published yet; in particular, decreasing the potential of the distal cluster of *E. coli* Hyd 1 had no effect on O_2 tolerance.[23]

Perspective

Chimeric dimers designed using the above described strategy will probably prove useful to evaluate the above hypotheses, for example in combination with site directed mutagenesis to separate the contributions of the whole subunits and individual residues.

It may also be hoped that once the subunits that define each catalytic property are identified, they can be assembled to produce dimers that simultaneously combine desirable features, such as tolerance to O_2 *and* bias in the direction of H_2 production. The chimeric dimer described here, in addition to being a useful new tool to study structure/function relationships, may therefore be the first of a new series of artificial enzymes with promising technological applications.[53,54]

Methods

Molecular biology and biochemistry. All strains, plasmids, oligonucleotides and purification procedures are described in detail in SI (sections S1 to S6).

Structural modeling. The structure of L1S2mod was calculated with ColabFold v1.5.2, AlphaFold2 using MMseqs2, and relaxed using amber force fields.[33]

Electrochemistry. The equipment was described before.[47,48] The solubilities of CO and O_2 in water were taken as 1 mM and 1.2 mM per atmosphere, respectively. The film of enzymes were made by polishing the surface of an home made pyrolytic graphite edge electrode (3 mm diameter) and drop casting 0.5 to 1 µL of protein solution (between 0.5 and 10 µM). For WT Hyd 1 and C19G/C120G Hyd 1, the films were also made by slow mass transport limited adsorption from the electrochemical cell solution, as described in ref [36]. All the experiments were performed in a buffer containing MES, CHES, HEPES, TAPS, Na acetate (each 5 mM), and NaCl (0.1 M).

Supporting information

Sections S1 to S6: bacterial strains and plasmids, oligonucleotides, construction of *E. coli* ΔS1 mutant, hydrogenase cloning and mutagenesis, culture growth conditions, biochemistry. Section S7: electrochemistry, including the quantitative assessment of the catalytic bias, measurement of the Michaelis constants, measurement of the CO inhibition constants, voltammetry of L1S2mod and L1S2mod1, comparison of the 100 and 3% H_2 CVs in main text fig. 2. Section S8: table showing the FeS cluster's redox potentials in NiFe hydrogenases. Section S9: structural analyses. The SI file is available free of charge at https://pubs.acs.org

Acknowledgements

This research was funded by the Centre National de la Recherche Scientifique, Aix Marseille Université, Agence Nationale de la Recherche (ANR-14-CE05-0010, ANR-18-CE05-0029), Région Sud. This work received support from the french government under the France 2030 investment plan, as part of the Initiative d'Excellence d'Aix-Marseille Université – A*MIDEX, AMX-22-RE-AB-097. The authors are very grateful to Frank Sargent (Newcastle University, UK) for providing the *E. coli* HJ001-hyp + pO^c and *E. coli* FTD147 strains, S. R. Kushner (University of Georgia, United States) for providing the pMAK705 plasmid; M. Menestreau and A. Latifi for the deletion of the *iscR* gene in *E. coli* FTD147 ; Frédérique Berger, glass blower at Aix Marseille University ; and the proteomic facility of the Institut de Microbiologie de la Méditerranée (IMM, CNRS-AMU, FR3479), Marseille Proteomique (MaP), for performing proteomic analyses by mass spectrometry.

References

(1) Stripp, S. T.; Duffus, B. R.; Fourmond, V.; Léger, C.; Leimkühler, S.; Hirota, S.; Hu, Y.; Jasniewski, A.; Ogata, H.; Ribbe, M. W. Second and Outer Coordination Sphere Effects in Nitrogenase, Hydrogenase, Formate Dehydrogenase, and CO Dehydrogenase. *Chem. Rev.* **2022**, *122* (14), 11900–11973. doi:10.1021/acs.chemrev.1c00914

(2) Fourmond, V.; Plumeré, N.; Léger, C. Reversible Catalysis. *Nature Reviews Chemistry* **2021**, *5* (5), 348–360. doi:10.1038/s41570-021-00268-3

(3) Dutta, A.; Appel, A. M.; Shaw, W. J. Designing Electrochemically Reversible H2 Oxidation and Production Catalysts. *Nature Reviews Chemistry* **2018**, *2* (9), 244–252. doi:10.1038/s41570-018-0032-8

(4) Cunningham, D. W.; Barlow, J. M.; Velasquez, R. S.; Yang, J. Reversible and Selective CO2 to HCO2- Electrocatalysis near the Thermodynamic Potential. *Angew. Chem. Int. Ed Engl.* **2019**, 59 (11), 4443-4447. doi:10.1002/anie.201913198

(5) Peters, J. W.; Schut, G. J.; Boyd, E. S.; Mulder, D. W.; Shepard, E. M.; Broderick, J. B.; King, P. W.; Adams, M. W. W. [FeFe]- and [NiFe]-Hydrogenase Diversity, Mechanism, and Maturation. *Biochim. Biophys. Acta* **2015**, *1853* (6), 1350–1369. doi:10.1016/j.bbamcr.2014.11.021

(6) Greening, C.; Biswas, A.; Carere, C. R.; Jackson, C. J.; Taylor, M. C.; Stott, M. B.; Cook, G. M.; Morales, S. E. Genomic and Metagenomic Surveys of Hydrogenase Distribution Indicate H2 Is a Widely Utilised Energy Source for Microbial Growth and Survival. *ISME J.* **2016**, *10* (3), 761–777. doi:10.1038/ismej.2015.153

(7) Page, C. C.; Moser, C. C.; Chen, X.; Dutton, P. L. Natural Engineering Principles of Electron Tunnelling in Biological Oxidation-Reduction. *Nature* **1999**, *402* (6757), 47–52. doi:10.1038/46972

(8) Leroux, F.; Dementin, S.; Burlat, B.; Cournac, L.; Volbeda, A.; Champ, S.; Martin, L.; Guigliarelli, B.; Bertrand, P.; Fontecilla-Camps, J.; Rousset, M.; Léger, C. Experimental Approaches to Kinetics of Gas Diffusion in Hydrogenase. *Proc. Natl. Acad. Sci. U. S. A.* **2008**, *105* (32), 11188–11193. doi:10.1073/pnas.0803689105
(9) Abou Hamdan, A.; Burlat, B.; Gutiérrez-Sanz, O.; Liebgott, P.-P.; Baffert, C.; De Lacey, A. L.; Rousset, M.; Guigliarelli, B.; Léger, C.; Dementin, S. O2-Independent Formation of the Inactive States of NiFe Hydrogenase. *Nat. Chem. Biol.* **2013**, *9* (1), 15–17. doi:10.1038/nchembio.1110
(10) Lukey, M. J.; Parkin, A.; Roessler, M. M.; Murphy, B. J.; Harmer, J.; Palmer, T.; Sargent, F.; Armstrong, F. A. How Escherichia Coli Is Equipped to Oxidize Hydrogen under Different Redox Conditions. *JBC* **2010**, *285* (6), 3928–3938. doi:10.1074/jbc.M109.067751
(11) Sargent, F. Chapter Eight - The Model [NiFe]-Hydrogenases of Escherichia Coli. In *Advances in Microbial Physiology*; Poole, R. K., Ed.; Academic Press, 2016; Vol. 68, pp 433–507. doi:10.1016/bs.ampbs.2016.02.008
(12) Beaton, S. E.; Evans, R. M.; Finney, A. J.; Lamont, C. M.; Armstrong, F. A.; Sargent, F.; Carr, S. B. The Structure of Hydrogenase-2 from Escherichia Coli: Implications for H2-Driven Proton Pumping. *Biochem. J* **2018**, *475* (7), 1353–1370. doi:10.1042/BCJ20180053
(13) Volbeda, A.; Amara, P.; Darnault, C.; Mouesca, J.-M.; Parkin, A.; Roessler, M. M.; Armstrong, F. A.; Fontecilla-Camps, J. C. X-Ray Crystallographic and Computational Studies of the O2-Tolerant [NiFe]-Hydrogenase 1 from Escherichia Coli. *Proc. Natl. Acad. Sci. U. S. A.* **2012**, *109* (14), 5305–5310. doi:10.1073/pnas.1119806109
(14) Fritsch, J.; Scheerer, P.; Frielingsdorf, S.; Kroschinsky, S.; Friedrich, B.; Lenz, O.; Spahn, C. M. T. The Crystal Structure of an Oxygen-Tolerant Hydrogenase Uncovers a Novel Iron-Sulphur Centre. *Nature* **2011**, *479* (7372), 249–252. doi:10.1038/nature10505
(15) Pandelia, M.-E.; Nitschke, W.; Infossi, P.; Giudici-Orticoni, M.-T.; Bill, E.; Lubitz, W. Characterization of a Unique [FeS] Cluster in the Electron Transfer Chain of the Oxygen Tolerant [NiFe] Hydrogenase from Aquifex Aeolicus. *Proc. Natl. Acad. Sci. U. S. A.* **2011**, *108* (15), 6097–6102. doi:10.1073/pnas.1100610108
(16) Frielingsdorf, S.; Fritsch, J.; Schmidt, A.; Hammer, M.; Löwenstein, J.; Siebert, E.; Pelmenschikov, V.; Jaenicke, T.; Kalms, J.; Rippers, Y.; Lendzian, F.; Zebger, I.; Teutloff, C.; Kaupp, M.; Bittl, R.; Hildebrandt, P.; Friedrich, B.; Lenz, O.; Scheerer, P. Reversible [4Fe-3S] Cluster Morphing in an O(2)-Tolerant [NiFe] Hydrogenase. *Nat. Chem. Biol.* **2014**, *10* (5), 378–385. doi:10.1038/nchembio.1500
(17) Fritsch, J.; Lenz, O.; Friedrich, B. The Maturation Factors HoxR and HoxT Contribute to Oxygen Tolerance of Membrane-Bound [NiFe] Hydrogenase in Ralstonia Eutropha H16. *J. Bacteriol.* **2011**, *193* (10), 2487 - 2497. doi:10.1128/JB.01427-10
(18) Lukey, M. J.; Roessler, M. M.; Parkin, A.; Evans, R. M.; Davies, R. A.; Lenz, O.; Friedrich, B.; Sargent, F.; Armstrong, F. A. Oxygen-Tolerant [NiFe]-Hydrogenases: The Individual and Collective Importance of Supernumerary Cysteines at the Proximal Fe-S Cluster. *J. Am. Chem. Soc.* **2011**, *133* (42), 16881–16892. doi:10.1021/ja205393w
(19) Rousset, M.; Montet, Y.; Guigliarelli, B.; Forget, N.; Asso, M.; Bertrand, P.; Fontecilla-Camps, J. C.; Hatchikian, E. C. [3Fe-4S] to [4Fe-4S] Cluster Conversion in *Desulfovibrio Fructosovorans* [NiFe] Hydrogenase by Site-Directed Mutagenesis. *Proc. Natl. Acad. Sci. U. S. A.* **1998**, *95* (20), 11625–11630. doi:10.1073/pnas.95.20.11625
(20) Evans, R. M.; Parkin, A.; Roessler, M. M.; Murphy, B. J.; Adamson, H.; Lukey, M. J.; Sargent, F.; Volbeda, A.; Fontecilla-Camps, J. C.; Armstrong, F. A. Principles of Sustained Enzymatic Hydrogen Oxidation in the Presence of Oxygen--the Crucial Influence of High Potential Fe-S Clusters in the Electron Relay of [NiFe]-Hydrogenases. *J. Am. Chem. Soc.* **2013**, *135* (7), 2694–2707. doi:10.1021/ja311055d
(21) Murphy, B. J.; Sargent, F.; Armstrong, F. A. Transforming an Oxygen-Tolerant [NiFe] Uptake Hydrogenase into a Proficient, Reversible Hydrogen Producer. *Energy Environ. Sci.* **2014**, *7* (4), 1426–1433. doi:10.1039/C3EE43652G
(22) Hexter, S. V.; Grey, F.; Happe, T.; Climent, V.; Armstrong, F. A. Electrocatalytic Mechanism of Reversible Hydrogen Cycling by Enzymes and Distinctions between the Major Classes of Hydrogenases. *Proc. Natl. Acad. Sci. U. S. A.* **2012**, *109* (29), 11516–11521. doi:10.1073/pnas.1204770109
(23) Adamson, H.; Robinson, M.; Wright, J. J.; Flanagan, L. A.; Walton, J.; Elton, D.; Gavaghan, D. J.; Bond, A. M.; Roessler, M. M.; Parkin, A. Retuning the Catalytic Bias and Overpotential of a [NiFe]-Hydrogenase via a Single Amino Acid Exchange at the Electron Entry/Exit Site. *J. Am. Chem. Soc.* **2017**, *139* (31), 10677–10686. doi:10.1021/jacs.7b03611
(24) Fourmond, V.; Baffert, C.; Sybirna, K.; Lautier, T.; Abou Hamdan, A.; Dementin, S.; Soucaille, P.; Meynial-Salles, I.; Bottin, H.; Léger, C. Steady-State Catalytic Wave-Shapes for 2-Electron Reversible Electrocatalysts and Enzymes. *J. Am. Chem. Soc.* **2013**, *135* (10), 3926–3938. doi:10.1021/ja311607s
(25) Flanagan, L. A.; Wright, J. J.; Roessler, M. M.; Moir, J. W.; Parkin, A. Re-Engineering a NiFe Hydrogenase to Increase the H2 Production Bias While Maintaining Native Levels of O2 Tolerance. *Chem. Commun.* **2016**, *52* (58), 9133–9136. doi:10.1039/c6cc00515b
(26) Goris, T.; Wait, A. F.; Saggu, M.; Fritsch, J.; Heidary, N.; Stein, M.; Zebger, I.; Lendzian, F.; Armstrong, F. A.; Friedrich, B.; Lenz, O. A Unique Iron-Sulfur Cluster Is Crucial for Oxygen Tolerance of a [NiFe]-Hydrogenase. *Nat. Chem. Biol.* **2011**, *7* (5), 310–318. doi:10.1038/nchembio.555
(27) Nishikawa, K.; Ogata, H.; Higuchi, Y. Structural Basis of the Function of [NiFe]-Hydrogenases. *Chem. Lett.* **2020**, *49* (2), 164–173. doi:10.1246/cl.190814
(28) Hartmann, S.; Frielingsdorf, S.; Ciaccafava, A.; Lorent, C.; Fritsch, J.; Siebert, E.; Priebe, J.; Haumann, M.; Zebger, I.; Lenz, O. O2-Tolerant H2 Activation by an Isolated Large Subunit of a [NiFe] Hydrogenase. *Biochemistry* **2018**, *57* (36), 5339–5349. doi:10.1021/acs.biochem.8b00760
(29) Pinske, C.; Krüger, S.; Soboh, B.; Ihling, C.; Kuhns, M.; Braussemann, M.; Jaroschinsky, M.; Sauer, C.; Sargent, F.; Sinz, A.;

Sawers, R. G. Efficient Electron Transfer from H2 to Benzyl Viologen by the NiFe-Hydrogenases of E. Coli Is Dependent on the Coexpression of the Iron-Sulfur Cluster-Containing Small Subunit. *Arch. Microbiol.* **2011**, *193* (12), 893–903. doi:10.1007/s00203-011-0726-5

(30) Léger, C.; Bertrand, P. Direct Electrochemistry of Redox Enzymes as a Tool for Mechanistic Studies. *Chem. Rev.* **2008**, *108* (7), 2379–2438. doi:10.1021/cr0680742

(31) Del Barrio, M.; Sensi, M.; Orain, C.; Baffert, C.; Dementin, S.; Fourmond, V.; Léger, C. Electrochemical Investigations of Hydrogenases and Other Enzymes That Produce and Use Solar Fuels. *Acc. Chem. Res.* **2018**, *51* (3), 769–777. doi:10.1021/acs.accounts.7b00622

(32) Inference of Macromolecular Assemblies from Crystalline State. *J. Mol. Biol.* **2007**, *372* (3), 774–797. doi:10.1016/j.jmb.2007.05.022

(33) Mirdita, M.; Schütze, K.; Moriwaki, Y.; Heo, L.; Ovchinnikov, S.; Steinegger, M. ColabFold: Making Protein Folding Accessible to All. *Nat. Methods* **2022**, *19* (6), 679–682. doi:10.1038/s41592-022-01488-1

(34) Sumner, I.; Voth, G. A. Proton Transport Pathways in [NiFe]-Hydrogenase. *J. Phys. Chem. B* **2012**, *116* (9), 2917–2926. doi:10.1021/jp208512y

(35) Teixeira, V. H.; Soares, C. M.; Baptista, A. M. Proton Pathways in a [NiFe]-Hydrogenase: A Theoretical Study. *Proteins* **2008**, *70* (3), 1010–1022. doi:10.1002/prot.21588

(36) Aldinio-Colbachini, A.; Fasano, A.; Guendon, C.; Bailly, A.; Wozniak, J.; Baffert, C.; Kpebe, A.; Léger, C.; Brugna, M.; Fourmond, V. Transport Limited Adsorption Experiments Give a New Lower Estimate of the Turnover Frequency of Escherichia Coli Hydrogenase 1. *BBA Advances* **2023**, 100090. doi:10.1016/j.bbadva.2023.100090

(37) del Barrio, M.; Guendon, C.; Kpebe, A.; Baffert, C.; Fourmond, V.; Brugna, M.; Léger, C. Valine-to-Cysteine Mutation Further Increases the Oxygen Tolerance of Escherichia Coli NiFe Hydrogenase Hyd-1. *ACS Catal.* **2019**, *9* (5), 4084–4088. doi:10.1021/acscatal.9b00543

(38) Redwood, M. D.; Mikheenko, I. P.; Sargent, F.; Macaskie, L. E. Dissecting the Roles of Escherichia Coli Hydrogenases in Biohydrogen Production. *FEMS Microbiol. Lett.* **2008**, *278* (1), 48–55. doi:10.1111/j.1574-6968.2007.00966.x

(39) Skibinski David A. G.; Golby Paul; Chang Yung-Sheng; Sargent Frank; Hoffman Ralf; Harper R.; Guest John R.; Attwood Margaret M.; Berks Ben C.; Andrews Simon C. Regulation of the Hydrogenase-4 Operon of Escherichia Coli by the σ54-Dependent Transcriptional Activators FhlA and HyfR. *J. Bacteriol.* **2002**, *184* (23), 6642–6653. doi:10.1128/JB.184.23.6642-6653.2002

(40) Weyman, P. D.; Vargas, W. A.; Chuang, R.-Y.; Chang, Y.; Smith, H. O.; Xu, Q. Heterologous Expression of Alteromonas Macleodii and Thiocapsa Roseopersicina [NiFe] Hydrogenases in Escherichia Coli. *Microbiology* **2011**, *157* (5), 1363–1374. doi:10.1099/mic.0.044834-0

(41) Sensi, M.; del Barrio, M.; Baffert, C.; Fourmond, V.; Léger, C. New Perspectives in Hydrogenase Direct Electrochemistry. *Current Opinion in Electrochemistry* **2017**, *5* (1), 135–145. doi:10.1016/j.coelec.2017.08.005

(42) Merrouch, M.; Hadj-Saïd, J.; Léger, C.; Dementin, S.; Fourmond, V. Reliable Estimation of the Kinetic Parameters of Redox Enzymes by Taking into Account Mass Transport towards Rotating Electrodes in Protein Film Voltammetry Experiments. *Electrochim. Acta* **2017**, *245*, 1059–1064. doi:10.1016/j.electacta.2017.03.114

(43) Fourmond, V.; Infossi, P.; Giudici-Orticoni, M.-T.; Bertrand, P.; Léger, C. Chronoamperometric Method for Studying the Anaerobic Inactivation of an Oxygen Tolerant NiFe Hydrogenase. *J. Am. Chem. Soc.* **2010**, *132* (13), 4848–4857. doi:10.1021/ja910685j

(44) Jones, A. K.; Lamle, S. E.; Pershad, H. R.; Vincent, K. A.; Albracht, S. P. J.; Armstrong, F. A. Enzyme Electrokinetics: Electrochemical Studies of the Anaerobic Interconversions between Active and Inactive States of Allochromatium Vinosum [NiFe]-Hydrogenase. *J. Am. Chem. Soc.* **2003**, *125* (28), 8505–8514. doi:10.1021/ja035296y

(45) Abou Hamdan, A.; Liebgott, P.-P.; Fourmond, V.; Gutiérrez-Sanz, O.; De Lacey, A. L.; Infossi, P.; Rousset, M.; Dementin, S.; Léger, C. Relation between Anaerobic Inactivation and Oxygen Tolerance in a Large Series of NiFe Hydrogenase Mutants. *Proc. Natl. Acad. Sci. U. S. A.* **2012**, *109* (49), 19916–19921. doi:10.1073/pnas.1212258109

(46) Léger, C.; Jones, A. K.; Roseboom, W.; Albracht, S. P. J.; Armstrong, F. A. Enzyme Electrokinetics: Hydrogen Evolution and Oxidation by Allochromatium Vinosum [NiFe]-Hydrogenase. *Biochemistry* **2002**, *41* (52), 15736–15746. doi:10.1021/bi026586e

(47) Léger, C.; Dementin, S.; Bertrand, P.; Rousset, M.; Guigliarelli, B. Inhibition and Aerobic Inactivation Kinetics of Desulfovibrio Fructosovorans NiFe Hydrogenase Studied by Protein Film Voltammetry. *JACS* **2004**, *126* (38), 12162-12172. doi:10.1021/ja046548d

(48) Orain, C.; Saujet, L.; Gauquelin, C.; Soucaille, P.; Meynial-Salles, I.; Baffert, C.; Fourmond, V.; Bottin, H.; Léger, C. Electrochemical Measurements of the Kinetics of Inhibition of Two FeFe Hydrogenases by O2 Demonstrate That the Reaction Is Partly Reversible. *J. Am. Chem. Soc.* **2015**, *137* (39), 12580–12587. doi:10.1021/jacs.5b06934

(49) Grinter, R.; Kropp, A.; Venugopal, H.; Senger, M.; Badley, J.; Cabotaje, P. R.; Jia, R.; Duan, Z.; Huang, P.; Stripp, S. T.; Barlow, C. K.; Belousoff, M.; Shafaat, H. S.; Cook, G. M.; Schittenhelm, R. B.; Vincent, K. A.; Khalid, S.; Berggren, G.; Greening, C. Structural Basis for Bacterial Energy Extraction from Atmospheric Hydrogen. *Nature* **2023**, *615*, 541–547. doi:10.1038/s41586-023-05781-7

(50) Abou Hamdan, A.; Dementin, S.; Liebgott, P.-P.; Gutierrez-Sanz, O.; Richaud, P.; De Lacey, A. L.; Rousset, M.; Bertrand, P.; Cournac, L.; Léger, C. Understanding and Tuning the Catalytic Bias of Hydrogenase. *JACS* **2012**, *134* (20), 8368–8371. doi:10.1021/ja301802r

(51) Fasano, A.; Land, H.; Fourmond, V.; Berggren, G.; Léger, C. Reversible or Irreversible Catalysis of H+/H2 Conversion by FeFe Hydrogenases. *J. Am. Chem. Soc.* **2021**, *143* (48), 20320–20325. doi:10.1021/jacs.1c09554

(52) Kalms, J.; Schmidt, A.; Frielingsdorf, S.; van der Linden, P.; von Stetten, D.; Lenz, O.; Carpentier, P.; Scheerer, P. Krypton Derivatization of an O2 -Tolerant Membrane-Bound [NiFe] Hydrogenase Reveals a Hydrophobic Tunnel Network for Gas Transport. *Angew. Chem. Int. Ed Engl.* **2016**, *55* (18), 5586–5590. doi:10.1002/anie.201508976
(53) Caserta, G.; Roy, S.; Atta, M.; Artero, V.; Fontecave, M. Artificial Hydrogenases: Biohybrid and Supramolecular Systems for Catalytic Hydrogen Production or Uptake. *Curr. Opin. Chem. Biol.* **2015**, *25*, 36–47. doi:10.1016/j.cbpa.2014.12.018
(54) Simmons, T. R.; Berggren, G.; Bacchi, M.; Fontecave, M.; Artero, V. Mimicking Hydrogenases: From Biomimetics to Artificial Enzymes. *Coord. Chem. Rev.* **2014**, *270-271*, 127–150. doi:10.1016/j.ccr.2013.12.018